Nucleon resonances in πN scattering up to energies $\sqrt{s} \leqslant 2.0$ GeV

Guan Yeu Chen,[1] S. S. Kamalov,[1,2,3] Shin Nan Yang,[1] D. Drechsel,[3] and L. Tiator[3]
[1]*Department of Physics and Center for Theoretical Sciences, National Taiwan University, Taipei 10617, Taiwan*
[2]*Bogoliubov Laboratory for Theoretical Physics, JINR, Dubna, RU-141980 Moscow Region, Russia*
[3]*Institut für Kernphyik, Universität Mainz, D-55099 Mainz, Germany*
(Received 10 April 2007; published 26 September 2007)

A meson-exchange model for pion-nucleon scattering was previously constructed using a three-dimensional reduction scheme of the Bethe-Salpeter equation for a model Lagrangian involving π, η, N, Δ, ρ, and σ fields. We thereby extend our previous work by including the ηN channel and all the πN resonances with masses $\sim$2 GeV, up to the F waves. The effects of the $\pi\pi N$ channels are taken into account by introducing an effective width in the resonance propagators. The extended model gives an excellent fit to both πN phase shifts and inelasticity parameters in all channels, except F_{17}, up to the F waves and for energies below 2 GeV. We present a new scheme for extracting the properties of overlapping resonances. The predicted values for the resonance masses and widths as well as resonance pole positions and residues are compared with the listing of the Particle Data Group.

DOI: 10.1103/PhysRevC.76.035206 PACS number(s): 13.75.Gx, 14.20.Gk, 11.80.Gw, 25.80.Dj

I. INTRODUCTION

Pion-nucleon scattering is of interest because of its fundamental nature. In the 1950s, it was widely regarded as *the* dynamical problem because of the special role pions and nucleons play in the family of particles [1]. Soon it became one of the main sources of information about the baryon spectrum. The pion-nucleon interaction also plays a fundamental role in the description of nuclear dynamics for which the πN off-shell amplitude serves as the basic input to most of the existing nuclear calculations at intermediate energies. Knowledge about the off-shell πN amplitude is also essential in interpreting the experiments performed at the intermediate-energy electron accelerators in order to unravel the internal structure of these hadrons. For example, the importance of the πN off-shell t matrix in a dynamical description of pion electromagnetic production has been demonstrated in recent years [2–5]. To make further progress, it is now necessary to improve our previous description of the πN interaction and to extend it to higher energies.

It is commonly accepted that quantum chromodynamics (QCD) is the fundamental theory of the strong interaction. However, due to the confinement problem, it is still practically impossible to derive the πN interaction directly from QCD. On the other hand, models based on meson-exchange pictures [6,7] have been very successful in describing the NN scattering. Over the last decade, similarly successful models have also been constructed for πN scattering [3,8–16]. Most of the recent attempts in this direction were obtained by applying various three-dimensional reductions of the Bethe-Salpeter equation, except for Ref. [12], in which the four-dimensional Bethe-Salpeter equation was solved. Because the effective Lagrangian used in these models includes only the first few low-lying resonances, in addition to pion and nucleon as well as σ and ρ mesons, the energy region is restricted to low and intermediate energies.

In previous works we constructed several meson-exchange πN models within the Bethe-Salpeter formulation [3,10,14] and investigated their sensitivity with respect to various three-dimensional reduction schemes. The model Lagrangian included only π, N, Δ, ρ, and σ fields, and it was found that all the resulting meson-exchange models can yield similarly good descriptions of the πN scattering data up to 400 MeV. The model obtained with the Cooper-Jennings reduction scheme [17] was recently extended up to a c.m. energy of 2 GeV in the S_{11} channel by including the ηN channel and a set of higher S_{11} resonances [18]. An excellent fit to the t matrix in both πN and ηN channels was obtained. In addition, when analyzing the pion photoproduction data, we obtained background contributions to the imaginary part of the S-wave multipole which differ considerably from the result based on the K-matrix approximation. The resulting resonance contributions required to explain the pion photoproduction data led to a substantial change of the extracted electromagnetic helicity amplitudes. In the present paper, we further extend our model to include the higher partial waves up to the F waves. The spin-$\frac{3}{2}$ resonances are treated as Rarita-Schwinger particles, while we use simple Breit-Wigner forms for the resonance propagators with spins $\frac{5}{2}$ and $\frac{7}{2}$. Since the importance of $\pi\pi N$ final states grows with energy, these channels also have to be taken care of. Instead of including them like the σN, ρN, and $\pi\Delta$ states directly in the coupled-channels calculation as done in Ref. [15], we follow the recipe of Ref. [18] to account for the $\pi\pi N$ channels by introducing a phenomenological term in the resonance propagators. It turns out that this approximation works quite well in most of the considered channels.

The question of whether a resonance is a three-quark state dressed by the meson cloud or is generated dynamically is an issue still under investigation in the literature. At one extreme, there is the conjecture [19] that baryon resonances not belonging to the large-N_c ground states may be generated by coupled-channel dynamics. On the other hand, in the Jülich πN model [20,21], it was found that only the Roper resonance $P_{11}(1440)$ can be understood in this way, while other resonances such as $S_{11}(1535)$, $S_{11}(1650)$, and $D_{13}(1520)$

had to be included in the model explicitly, in direct contrast to results of Ref. [9], where Roper resonance is included explicitly but $S_{11}(1535)$ is generated dynamically. Here we take another extreme and assume all the nucleon resonances are fundamentally three-quark states dressed by coupling to meson-nucleon channels. Such a picture has been found to describe well the $\Delta(1232)$ [5,22,23] and S_{11} resonances up to 2 GeV [18] in πN scattering and pion electromagnetic production.

In Sec. II, we summarize the meson-exchange πN model constructed in our previous work. We extend the model to include the ηN channel and the higher resonances in Sec. III. Our results are presented in Sec. IV, and some conclusions are given in Sec. V.

II. MESON-EXCHANGE πN MODEL

Let us first outline the content of our previous meson-exchange model describing the πN interaction at low and intermediate energies [14]. The reaction of interest is

$$\pi(q) + N(p) \to \pi(q') + N(p'), \tag{1}$$

where q, p, q', and p' are the four-momenta of the respective particles. We further define the total and relative four-momentum, $P = p + q$ and $k = p\eta_\pi(s) - q\eta_N(s)$, respectively, where $s = P^2 = W^2$ is the Mandelstam variable. The dimensionless variables $\eta_\pi(s)$ and $\eta_N(s)$ represent the freedom in choosing a three-dimensional reduction and are constrained by the condition $\eta_N + \eta_\pi = 1$. An often used definition for these variables is given by

$$\eta_N(s) = \frac{\varepsilon_N(s)}{\varepsilon_N(s) + \varepsilon_\pi(s)}, \quad \eta_\pi(s) = \frac{\varepsilon_\pi(s)}{\varepsilon_N(s) + \varepsilon_\pi(s)}, \tag{2}$$

with $\varepsilon_N(s) = (s + m_N^2 - m_\pi^2)/2\sqrt{s}$ and $\varepsilon_\pi(s) = (s - m_N^2 + m_\pi^2)/2\sqrt{s}$. For further details, we refer the reader to Ref. [14].

The Bethe-Salpeter (BS) equation for πN scattering takes the general form

$$T_{\pi N} = B_{\pi N} + B_{\pi N} G_0 T_{\pi N}, \tag{3}$$

where $B_{\pi N}$ is the sum of all irreducible two-particle Feynman amplitudes and G_0 the free relativistic pion-nucleon propagator. The BS equation can be cast into the form

$$T_{\pi N} = \hat{B}_{\pi N} + \hat{B}_{\pi N} \hat{G}_0 T_{\pi N}, \tag{4}$$

with

$$\hat{B}_{\pi N} = B_{\pi N} + B_{\pi N}(G_0 - \hat{G}_0)\hat{B}_{\pi N}, \tag{5}$$

where a three-dimensional reduction of Eq. (3) is obtained by use of an appropriate propagator $\hat{G}_0(k; P)$. It is also convenient to choose $\hat{G}_0$ such that two-body unitarity is maintained by reproducing the πN elastic cut. There is still a wide range of possible propagators which satisfy this requirement. A standard choice of the propagator has the form [17,24]

$$\begin{aligned}\hat{G}_0(k; P) = \frac{1}{(2\pi)^3} \int \frac{ds'}{s - s'} f(s, s')[\alpha(s, s')\not{P}' + \not{k} + m_N] \\ \times \delta^{(+)}\big([\eta_N(s')P' + k]^2 - m_N^2\big) \\ \times \delta^{(+)}\big([\eta_\pi(s')P' - k]^2 - m_\pi^2\big),\end{aligned} \tag{6}$$

with $P' = \sqrt{\frac{s'}{s}}P$. The superscript $(+)$ associated with δ functions signifies that only the positive energy part is kept in the propagator. Concerning the Dirac matrices and the Lorentz metrics, we use the notation of Bjorken and Drell [25]. Furthermore, the variables f and α are dimensionless variables containing the freedom of reduction; they are constrained by the conditions $f(s, s) = 1$ and $\alpha(s, s) = \eta_N(s)$, which ensure the reproduction of the elastic cut. In the Cooper-Jennings reduction scheme [17], they take the form

$$\alpha(s, s') = \eta_N(s), \quad f(s, s') = \frac{4\sqrt{ss'}\varepsilon_N(s')\varepsilon_\pi(s')}{ss' - (m_N^2 - m_\pi^2)^2}. \tag{7}$$

The integral over s' in Eq. (6) can be performed. Expressed in the c.m. frame, the result is

$$\begin{aligned}\hat{G}_0(k; s) = \frac{1}{(2\pi)^3} \frac{\delta(k_0 - \hat{\eta}(s_{\vec{k}}, \vec{k}))}{\sqrt{s} - \sqrt{s_{\vec{k}}}} \frac{2\sqrt{s_{\vec{k}}}}{\sqrt{s} + \sqrt{s_{\vec{k}}}} f(s, s_{\vec{k}}) \\ \times \frac{\alpha(s, s_{\vec{k}})\gamma_0\sqrt{s} + \not{k} + m_N}{4E_N(\vec{k})E_\pi(\vec{k})},\end{aligned} \tag{8}$$

where $E_N(\vec{k})$ and $E_\pi(\vec{k})$ are the nucleon and pion energies for the three-momentum $\vec{k}$, $\sqrt{s_{\vec{k}}} = E_N(\vec{k}) + E_\pi(\vec{k}) = E$ is the total energy in the c.m. frame, and $\hat{\eta}(s, \vec{k}) = E_N(\vec{k}) - \eta_N(s_{\vec{k}})\sqrt{s_{\vec{k}}}$. By use of these relations, we obtain the following πN scattering equation:

$$\begin{aligned}t(\vec{k}', \vec{k}; E) = v(\vec{k}', \vec{k}; E) + \int d\vec{k}'' v(\vec{k}', \vec{k}''; E) g_0(\vec{k}''; E) \\ \times t(\vec{k}'', \vec{k}; E).\end{aligned} \tag{9}$$

The explicit relations between the variables of Eqs. (9) and (3) are

$$\begin{aligned}t(\vec{k}', \vec{k}; E) &= \int dk_0' dk_0 \delta(k_0' - \hat{\eta}')T(k', k; E)\delta(k_0 - \hat{\eta}), \\ v(\vec{k}', \vec{k}; E) &= \int dk_0' dk_0 \delta(k_0' - \hat{\eta}')B(k', k; E)\delta(k_0 - \hat{\eta}), \\ g_0(\vec{k}; E) &= \int dk_0 \hat{G}_0(k; E),\end{aligned} \tag{10}$$

with $\hat{\eta}' = \hat{\eta}(s_{\vec{k}'}, \vec{k}')$ and $\hat{\eta} = \hat{\eta}(s_{\vec{k}}, \vec{k})$.

Because our previous work concentrated on the πN scattering process at low and intermediate energies, we only considered the degrees of freedom due to the π, N, σ, ρ, and $\Delta(1232)$ fields, and we approximated the sum of all irreducible two-particle Feynman amplitudes, $B(k', k; E)$ in Eq. (10), by the tree approximation of the following interaction Lagrangian:

$$\begin{aligned}\mathcal{L}_I = &\frac{f_{\pi NN}^{(0)}}{m_\pi} \bar{N}\gamma_5\gamma_\mu \vec{\tau} \cdot \partial^\mu \vec{\pi} N - g_{\sigma\pi\pi}^{(s)} m_\pi \sigma(\vec{\pi} \cdot \vec{\pi}) \\ &- \frac{g_{\sigma\pi\pi}^{(v)}}{2m_\pi} \sigma(\partial^\mu \vec{\pi} \cdot \partial_\mu \vec{\pi}) - g_{\sigma NN} \bar{N}\sigma N \\ &- g_{\rho NN} \bar{N} \left\{ \gamma_\mu \vec{\rho}^\mu + \frac{\kappa_V^\rho}{4m_N} \sigma_{\mu\nu}(\partial^\mu \vec{\rho}^\nu - \partial^\nu \vec{\rho}^\mu) \right\} \cdot \frac{1}{2}\vec{\tau} N \\ &- g_{\rho\pi\pi} \vec{\rho}^\mu \cdot (\vec{\pi} \times \partial_\mu \vec{\pi})\end{aligned}$$

$$-\frac{g_{\rho\pi\pi}}{4m_\rho^2}(\delta-1)(\partial^\mu\vec{\rho}^\nu-\partial^\nu\vec{\rho}^\mu)\cdot(\partial_\mu\vec{\pi}\times\partial_\nu\vec{\pi})$$
$$+\frac{g_{\pi N\Delta}}{m_\pi}\bar{\Delta}_\mu\left[g^{\mu\nu}-\left(Z+\frac{1}{2}\right)\gamma^\mu\gamma^\nu\right]\vec{T}_{\Delta N}N\cdot\partial_\nu\vec{\pi}, \tag{11}$$

with Δ_μ the Rarita-Schwinger field operator for the Δ resonance and $\vec{T}_{\Delta N}$ the isospin transition operator between the nucleon and the Δ. The resulting driving term consists of the direct and crossed N and Δ diagrams as well as the t-channel σ- and ρ-exchange contributions.

The procedure of Afnan and collaborators [26] was followed to constrain the P_{11} phase shift by imposing the nucleon pole condition. This treatment leads to a proper renormalization of both nucleon mass and πNN coupling constant. It also yields the important cancellation between the repulsive nucleon pole contribution and the attractive background, such that a reasonable fit to the πN phase shifts in the P_{11} channel can be achieved.

To complete the model, we further introduced form factors to regularize the driving term $v(\vec{k},\vec{k}')$ of Eq. (10). For this purpose, covariant form factors of the form

$$F(p^2)=\left[\frac{n\Lambda^4}{n\Lambda^4+(m^2-p^2)^2}\right]^n, \tag{12}$$

are associated with each leg of the vertices, where p is the four-momentum and m the mass of the respective particle. This parametrization is similar to the prescription of Ref. [8], and in Ref. [14] both $n=10$ and 2 were considered. However, in our previous work, we used the value $n=10$ [18].

The parameters that were allowed to vary in fitting the empirical phase shifts are the products $g_{\sigma NN}g^{(s)}_{\sigma\pi\pi}$, $g_{\sigma NN}g^{(v)}_{\sigma\pi\pi}$, and $g_{\rho NN}g_{\rho\pi\pi}$ as well as δ for the t-channel σ and ρ exchanges, $m^{(0)}_\Delta$, $g^{(0)}_{\pi N\Delta}$, and Z for the Δ mechanism, and the cutoff parameters Λ of the form factors given by Eq. (12). In the crossed N diagram, the physical πNN coupling constant is used. For the crossed Δ diagram, the situation is not so clear, since the determination of the "physical" $\pi N\Delta$ coupling constant depends on the nonresonant contribution in the P_{33} channel. In principle, it can be determined by carrying out a renormalization procedure similar to that used for the nucleon. However, this would require a much more difficult numerical task, because the Δ pole is complex. In accordance with Refs. [3,8,9], we therefore did not carry out such a renormalization for the Δ but simply determined the coupling constant in the crossed Δ diagram by a fit to the data. The resulting coupling constant was denoted as $g_{\pi N\Delta}$.

III. EXTENSION TO HIGHER ENERGIES: INCLUSION OF THE ηN CHANNEL AND HIGHER RESONANCES

As the energy increases, two-pion channels such as σN, ηN, $\pi\Delta$, ρN as well as a nonresonant continuum of $\pi\pi N$ states become increasingly important; at the same time, more and more nucleon resonances appear as intermediate states. The πN model described in Sec. II was therefore extended for the S_{11} partial wave by explicitly coupling the π, η, and $\pi\pi$ channels and including the couplings with higher baryon resonances [18]. In particular, in the case of only one contributing resonance R, the Hilbert space was enlarged by the inclusion of a bare S_{11} resonance R which acquires a width by its coupling with the πN and ηN channels through the Lagrangian

$$\mathcal{L}_\mathcal{I}=ig^{(0)}_{\pi NR}\bar{R}\tau N\cdot\pi+ig^{(0)}_{\eta NR}\bar{R}N\eta+\text{h.c.}, \tag{13}$$

where N, R, π, and η denote the field operators for the nucleon, bare resonance R, pion, and η meson, respectively. The full t matrix can be written as a system of coupled equations,

$$t_{ij}(E)=v_{ij}(E)+\sum_k v_{ik}(E)g_k(E)t_{kj}(E), \tag{14}$$

with i and j denoting the π and η channels and $E=W$ is the total c.m. energy.

In general, the potential v_{ij} is the sum of nonresonant (v^B_{ij}) and bare resonance (v^R_{ij}) terms,

$$v_{ij}(E)=v^B_{ij}(E)+v^R_{ij}(E). \tag{15}$$

The nonresonant term $v^B_{\pi\pi}$ for the πN elastic channel is given by the results of Sec. II and contains contributions from the s and u channels, Born terms, and t-channel contributions with ω, ρ, and σ exchange. The parameters in $v^B_{\pi\pi}$ are fixed from the analysis of the pion scattering phase shifts for the s and p waves at low energies ($W<1300$ MeV) [14]. In channels involving the η, the potential $v^B_{i\eta}$ is taken to be zero, because the ηNN coupling is very small [27].

The bare resonance contribution arises from the excitation and deexcitation of the resonance R,

$$v^R_{ij}(E)=\frac{h^{(0)\dagger}_{iR}h^{(0)}_{jR}}{E-M^{(0)}_R}, \tag{16}$$

where $h^{(0)}_{iR}$ and $M^{(0)}_R$ denote the bare vertex operator for $R\to\pi/\eta+N$ and the bare mass of the resonance R, respectively. The matrix elements of the potential $v^R_{ij}(E)$ can be symbolically expressed in the form

$$v^R_{ij}(q,q';E)=\frac{f_i(\tilde{\Lambda}_i,q;E)g^{(0)}_i g^{(0)}_j f_j(\tilde{\Lambda}_j,q';E)}{E-M^{(0)}_R+\frac{i}{2}\Gamma^{2\pi}_R(E)}, \tag{17}$$

where q and q' are the pion (or η) momenta in the initial and final states, and $g^{(0)}_{i/j}$ is the resonance vertex couplings. As in Ref. [14], we associate with each external line of the particle α in a πNR vertex a covariant form factor $F_\alpha=[n\Lambda^4_\alpha/\left(n\Lambda^4_\alpha+(p^2_\alpha-m^2_\alpha)^2\right)]^n$, where p_α, m_α, and Λ_α are the four-momentum, mass, and cutoff parameter of particle α, respectively, and $n=10$. As a result, f_i depends on the product of three cutoff parameters, i.e., $\tilde{\Lambda}_\pi\equiv(\Lambda_N,\Lambda_R,\Lambda_\pi)$.

In Eq. (17) we have included a phenomenological term $\Gamma^{2\pi}_R(E)$ in the resonance propagator to account for the $\pi\pi N$ decay channel. Therefore, our "bare" resonance propagator already contains some renormalization or "dressing" effects due to the coupling with the $\pi\pi N$ channel. With this prescription, we assume that any further nonresonant coupling mechanism with the $\pi\pi N$ channel is small. Following

Refs. [28,29], we take

$$\Gamma_R^{2\pi}(E) = \Gamma_R^{2\pi(0)} \left(\frac{q_{2\pi}}{q_0}\right)^{2l+4} \left(\frac{X_R^2 + q_0^2}{X_R^2 + q_{2\pi}^2}\right)^{l+2}, \quad (18)$$

where l is the pion orbital momentum, $q_{2\pi} = q_{2\pi}(E)$ the momentum of the compound two-pion system, $q_0 = q_{2\pi}(E = M_R^{(0)})$, and the quantity $\Gamma_R^{2\pi(0)}$ is the 2π decay width at resonance. We note that this form accounts for the correct energy behavior of the phase space near the three-body threshold [28]. In our present work, $\Gamma_R^{2\pi(0)}$ and X_R are considered as free parameters. As a result, one isolated resonance will in general contain six free parameters, the bare mass $M_R^{(0)}$, the decay width $\Gamma_R^{2\pi(0)}$, two bare coupling constants $g_i^{(0)}$ and $g_j^{(0)}$, and two cutoff parameters Λ_R and X_R. The generalization of the coupled-channels model to the case of N resonances with the same quantum numbers is then given by

$$v_{ij}^R(q, q'; E) = \sum_{n=1}^{N} v_{ij}^{R_n}(q, q'; E), \quad (19)$$

with free parameters for the bare masses, widths, coupling constants, and cutoff parameters for each resonance.

Having solved the coupled-channels equations, our next task is the extraction of the physical (or "dressed") masses, partial widths, and branching ratios of the resonances. It is known that this procedure is model dependent, because the background and the resonance contributions cannot be separated in a unique way. Of course, the solution to this problem becomes more and more difficult with an increasing number of overlapping resonances in the same channel. In the literature, there are two schemes used to separate the total t matrix into background and resonance contributions. For simplicity, we illustrate these two methods for the uncoupled channel case, i.e., assuming that only the πN channel is open. In this case, the potential operator describing the excitation of a bare resonance R takes the form

$$v_{\pi N}^R(E) = \frac{h_{\pi R}^{(0)\dagger} h_{\pi R}^{(0)}}{E - M_R^{(0)}}, \quad (20)$$

with $h_{\pi R}^{(0)}$ the bare vertex.

The first scheme was suggested by Afnan and collaborators [30] and recently used in the dynamical model calculation of pion scattering and pion photoproduction [4]. By use of the two-potential formulation, the t matrix is written as

$$t_{\pi N}(E) = \tilde{t}_{\pi N}^B(E) + \tilde{t}_{\pi N}^R(E), \quad (21)$$

where $\tilde{t}_{\pi N}^B(E)$ is defined as

$$\tilde{t}_{\pi N}^B(E) = v_{\pi N}^B + v_{\pi N}^B g_0(E) \tilde{t}_{\pi N}^B(E). \quad (22)$$

We will call $\tilde{t}_{\pi N}^B(E)$ the nonresonant background, because it does not contain any resonance contribution from $v_{\pi N}^R$ of Eq. (20). The resonance term $\tilde{t}_{\pi N}^R(E)$ takes the form

$$\tilde{t}_{\pi N}^R(E) = \bar{h}_{\pi R}(E) \frac{1}{E - M_R^{(0)} - \Sigma_R(E)} h_{\pi R}(E), \quad (23)$$

with the definitions

$$h_{\pi R}(E) = h_{\pi R}^{(0)} + h_{\pi R}^{(0)} g_0(E) \tilde{t}_{\pi N}^B(E), \quad (24)$$

$$\bar{h}_{\pi R}(E) = h_{\pi R}^{(0)\dagger} + \tilde{t}_{\pi N}^B(E) g_0(E) h_{\pi R}^{(0)\dagger}, \quad (25)$$

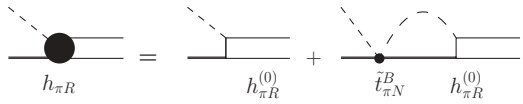

FIG. 1. Dressed and bare $\pi N R$ vertex.

and the self-energy $\Sigma_R(E)$ given by

$$\Sigma_R(E) = h_{\pi R}^{(0)} g_0 \bar{h}_{\pi R}(E) = h_{\pi R}^{(0)} g_0 h_{\pi R}^{(0)\dagger} + h_{\pi R}^{(0)} g_0 \tilde{t}_{\pi N}^B(E) g_0 h_{\pi R}^{(0)\dagger}. \quad (26)$$

Graphical representations of the dressed vertex $h_{\pi R}(E)$ and the self-energy $\Sigma_R(E)$ are depicted in Figs. 1 and 2, respectively, where the solid circle on the left-hand side of Fig. 1 denotes the dressed vertex $h_{\pi R}$, while the $\pi N R$ vertices, $h_{\pi R}^{(0)}$, on the right-hand side of Fig. 1 correspond to the excitation of a bare resonance R. The small solid circles in Figs. 1 and 2 represent the nonresonant background $\tilde{t}_{\pi N}^B(E)$ as defined in Eq. (22).

The information about the physical mass and total width of the resonance R is contained in the dressed resonance propagator given in Eq. (23). The complex self-energy $\Sigma(E)$ leads to a shift from the real "bare" mass to a complex and energy-dependent value. However, we characterize the resonances by energy-independent parameters obtained by solving the equation

$$E - M_R^{(0)} - \mathrm{Re}\,\Sigma_R(E) = 0. \quad (27)$$

The solution of this equation, $E = M_R$, corresponds to the energy at which the dressed propagator in Eq. (23) becomes purely imaginary and is used to define the physical or dressed mass,

$$M_R = M_R^{(0)} + \mathrm{Re}\,\Sigma_R(M_R), \quad (28)$$

and the width of the resonance,

$$\Gamma_R(M_R) = -2\,\mathrm{Im}\Sigma_R(M_R). \quad (29)$$

All of the above equations are based on the two-potential formulation [31]. The extension of this method to the case of several overlapping resonances in the same partial channel α complicates the problem. In particular, we cannot express the t matrix as a simple sum of a smooth background and overlapping resonances,

$$t_{\pi N}(E) \neq \tilde{t}_{\pi N}^B(E) + \sum_{i=1}^{N} \tilde{t}_{\pi N}^{R_i}(E). \quad (30)$$

We therefore prefer to separate the resonance and background contributions in the framework of Refs. [5,18]. In this approach, the full pion-nucleon scattering matrix is decomposed into

$$t_{\pi N}(E) = t_{\pi N}^B(E) + t_{\pi N}^R(E), \quad (31)$$

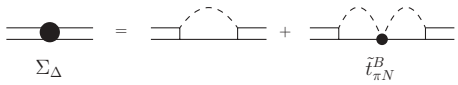

FIG. 2. Resonance self-energy.

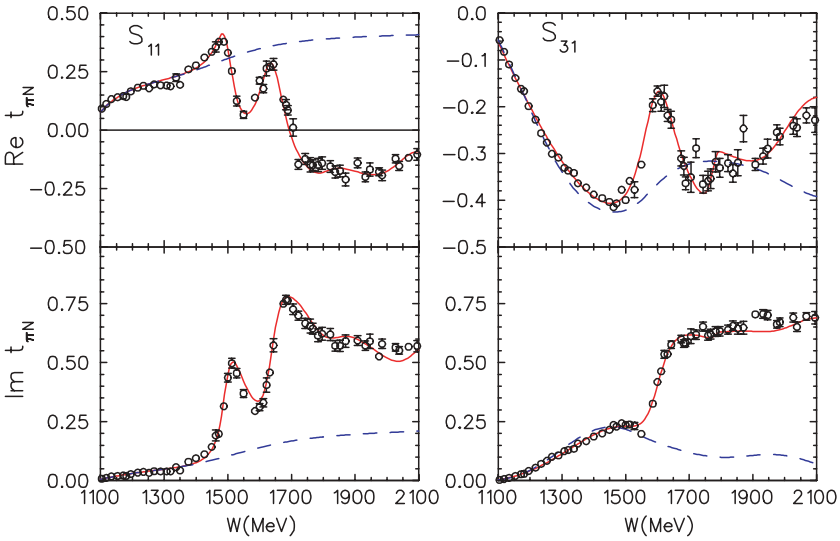

FIG. 3. (Color online) Real and imaginary parts of $t_{\pi N}$ in the S waves as function of the total c.m. energy W. The solid (red) lines are the best fits of our meson-exchange model, the dashed (blue) lines correspond to the contributions of the nonresonant background $\tilde{t}^B_{\pi N}$ of Eq. (22). The open circles are the results of the partial wave analysis of Ref. [34].

where

$$t^B_{\pi N}(E) = v^B_{\pi N} + v^B_{\pi N} g_0(E) t_{\pi N}(E), \tag{32}$$

$$t^R_{\pi N}(E) = v^R_{\pi N} + v^R_{\pi N} g_0(E) t_{\pi N}(E). \tag{33}$$

Comparing $t^B_{\pi N}$ with $\tilde{t}^B_{\gamma\pi}$ of Eq. (22), the background $t^B_{\pi N}$ now includes contributions not only from the background rescattering but also from intermediate resonance excitation. This is compensated by the fact that the resonance contribution

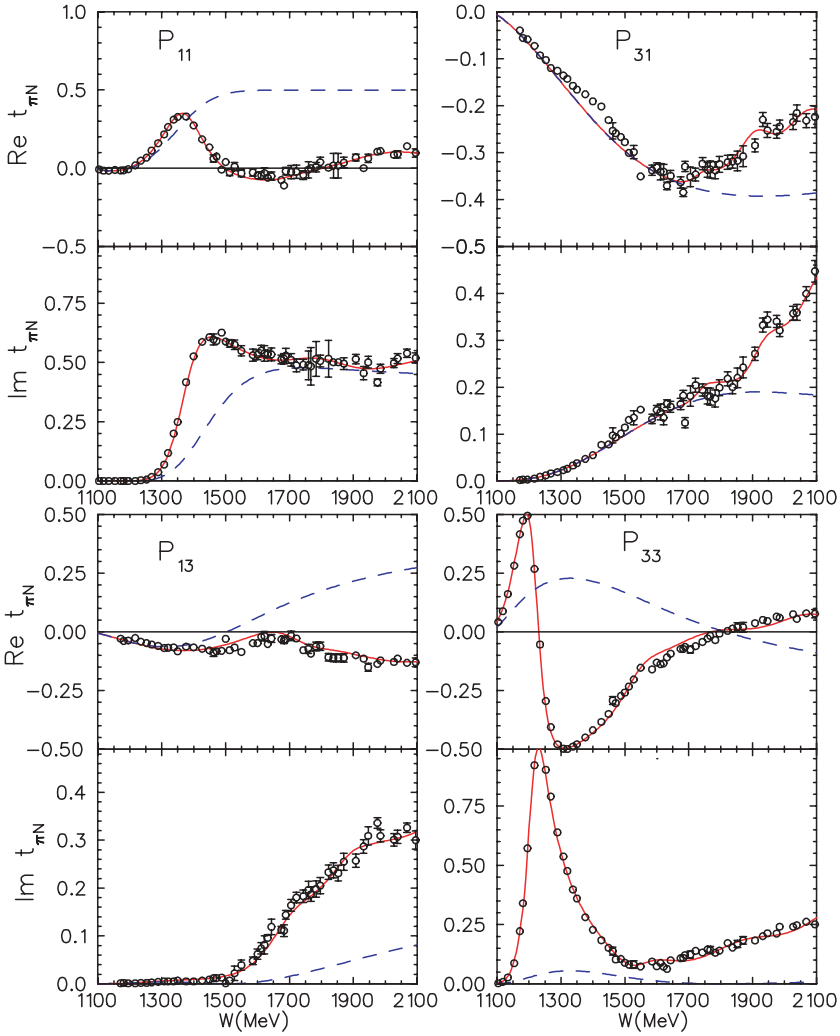

FIG. 4. (Color online) Same as Fig. 3, but for P waves.

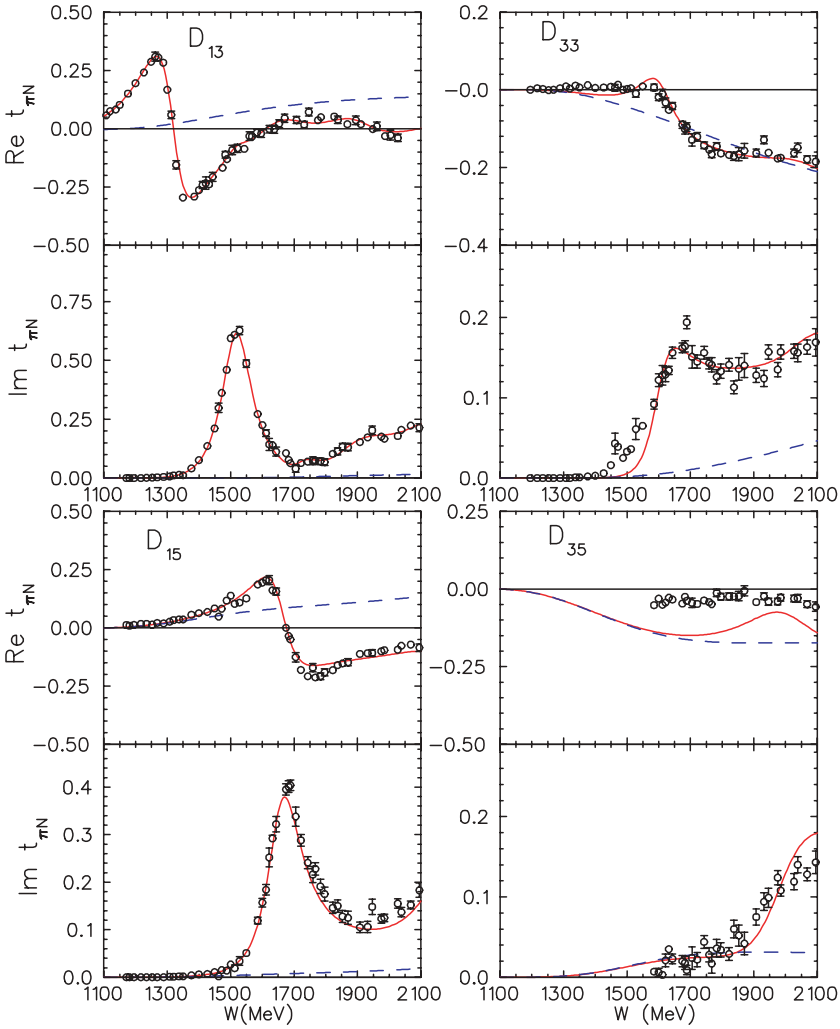

FIG. 5. (Color online) Same as Fig. 3, but for D waves.

$t^R_{\pi N}$ now contains only the terms that start with the bare resonance excitation. Expressed in terms of self-energy and vertex functions, we obtain the result

$$t^R_{\pi N}(E) = \frac{\bar{h}_{\pi R}(E) h^{(0)}_{\pi R}}{E - M^{(0)}_R(E) - \Sigma_R(E)}, \tag{34}$$

which differs from Eq. (23), where dressed vertex appears in both the initial and final states. On the other hand, we note that the resonance propagators of the two approaches are identical. Therefore, the physical masses and total widths determined in the two methods will be the same.

The second method can be easily extended to the case of N overlapping resonances by the following decomposition of the full πN scattering matrix into background and resonance contributions,

$$t_{\pi N}(E) = t^B_{\pi N}(E) + \sum_{i=1}^{N} t^{R_i}_{\pi N}(E). \tag{35}$$

The contribution from each resonance R_i can be expressed in terms of the bare $h^{(0)}_{\pi R_i}$ and dressed $h_{\pi R_i}(E)$ vertex operators as well as the resonance self-energy derived from one-pion $\Sigma^{1\pi}_{R_i}(E)$ and two-pion $\Sigma^{2\pi}_{R_i}(E)$ channels, that is,

$$t^{R_i}_{\pi N}(E) = \frac{\bar{h}_{\pi R_i}(E) h^{(0)}_{\pi R_i}}{E - M^{(0)}_{R_i} - \Sigma^{1\pi}_{R_i}(E) - \Sigma^{2\pi}_{R_i}(E)}, \tag{36}$$

where $M^{(0)}_{R_i}$ is the bare mass of the ith resonance. The contribution from the two-pion channel, $\Sigma^{2\pi}_{R_i}$, is defined phenomenologically as in Eq. (18). The vertices for the resonance excitation are obtained from the equations

$$h_{\pi R_i}(E) = h^{(0)}_{\pi R_i} + h^{(0)}_{\pi R_i} g_0(E) t^{B_i}_{\pi N}(E), \tag{37}$$

$$\bar{h}_{\pi R_i}(E) = h^{(0)\dagger}_{\pi R_i} + t^{B_i}_{\pi N}(E) g_0(E) h^{(0)\dagger}_{\pi R_i}, \tag{38}$$

where

$$t^{B_i}_{\pi N}(E) = v_i(E) + v_i(E) g_0(E) t^{B_i}_{\pi N}(E), \tag{39}$$

$$v_i(E) = v^B_{\pi N} + \sum_{j \neq i}^{N} v^{R_j}_{\pi N}(E), \tag{40}$$

with $v^{R_j}_{\pi N}(E)$ arising from the excitation of the resonance R_j as given in Eq. (17). The one-pion self-energies arising from

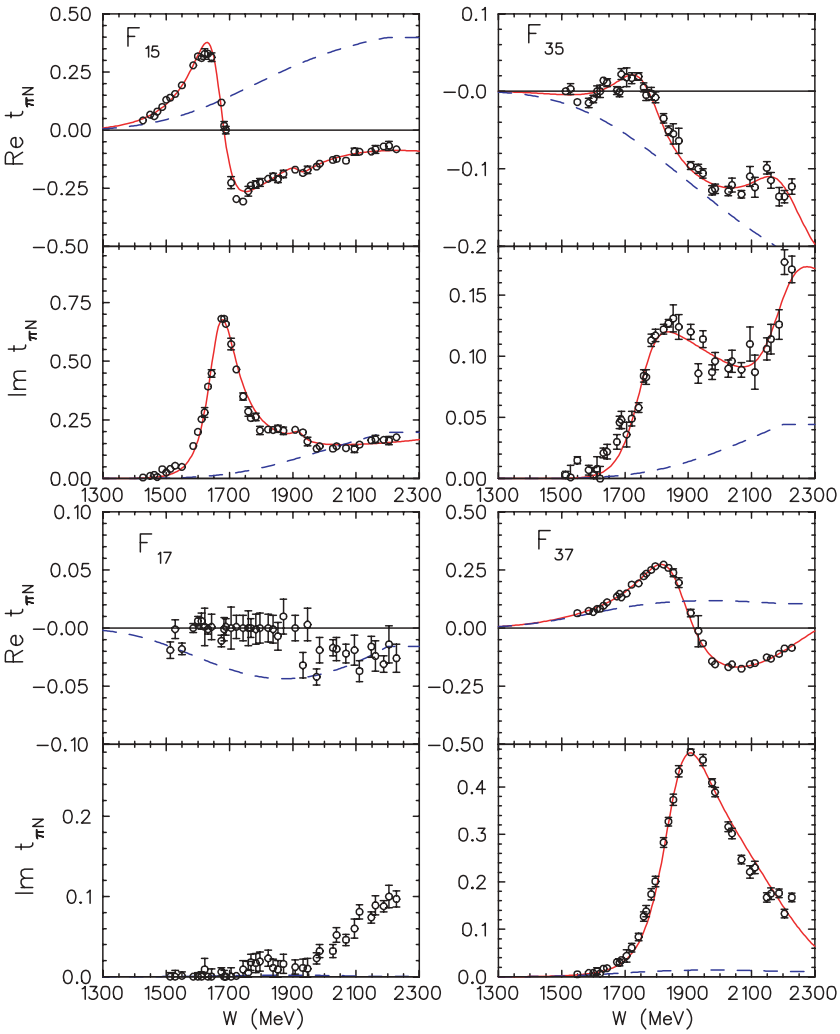

FIG. 6. (Color online) Same as Fig. 3, but for F waves.

$t^{B_i}_{\pi N}(E)$ of Eq. (39) are given as

$$\Sigma^{1\pi}_{R_i}(E) = h^{(0)}_{\pi R_i} g_0 \bar{h}_{\pi R_i}(E) = h^{(0)}_{\pi R_i} g_0 h^{(0)\dagger}_{\pi R_i} + h^{(0)}_{\pi R_i} g_0 t^{B_i}_{\pi N} g_0 h^{(0)\dagger}_{\pi R_i}, \quad (41)$$

and the one-pion branching ratio at the dressed resonance is

$$\beta^{1\pi}_i = \frac{\Sigma^{1\pi}_{R_i}(M_R)}{\Sigma^{1\pi}_{R_i}(M_R) + \Sigma^{2\pi}_{R_i}(M_R)}. \quad (42)$$

The pole positions in the complex energy plane and the complex residues of the scattering amplitudes at these poles are calculated using the speed plot technique for the pion-nucleon partial waves. For details, see Refs. [32,33]. We add in passing that in the case of broad and overlapping resonances and close-by thresholds, the speed-plot technique can lead to numerical uncertainties. In extreme cases, a pole may not be found at all.

Finally, it is not difficult to see from Eqs. (37) and (38) that the matrix elements of both $h_{\pi R_i}$ and $t^{B_i}_{\pi N}(E)$ would have the same phase $\phi_R(E)$, i.e.,

$$\langle h_{\pi R_i}(E)\rangle = |\langle h_{\pi R_i}(E)\rangle| \exp(i\phi_{R_i}), \quad \langle t^{B_i}_{\pi N}(E)\rangle = |\langle t^{B_i}_{\pi N}(E)\rangle| \exp(i\phi_{R_i}), \quad (43)$$

where the brackets $\langle\,\rangle$ are used to denote a matrix element of the operator sandwiched between the same set of initial and final states. It then follows that also the numerator on the right-hand side of Eq. (36) carries the phase $\phi_{R_i}(E)$. Information about this phase is very important for the phenomenological Breit-Wigner parametrization of the resonance contributions.

We emphasize that in the formulation of Eqs. (35)–(41), the nucleon resonances are treated in a completely symmetrical way. In addition, the self-energy and dressing of any resonance receive contributions from all other resonances.

IV. RESULTS AND DISCUSSION

A. πN scattering amplitudes

With the extended meson-exchange model described in Sec. III, we have fitted the πN phase shifts and inelasticity

TABLE I. Bare ($M_R^{(0)}$) and physical (M_R) resonance masses as well as total widths Γ_R, all in units of MeV, single pion branching ratios $\beta_R^{1\pi}$, and background phases ϕ_R of Eq. (43) for isospin-1/2 resonances. Upper lines: our results, lower lines: results of the PDG [35].

N^*	$M_R^{(0)}$	M_R	Γ_R	$\beta_R^{1\pi}(\%)$	ϕ_R (deg)
$P_{11}(1440)$	1612	1418	436	44	32
****		1445 ± 25	325 ± 125	65 ± 10	
$D_{13}(1520)$	1590	1520	94	62	1.2
****		1520 ± 5	115 ± 15	60 ± 5	
$S_{11}(1535)$	1559	1520	130	43	20
****		1535 ± 10	150 ± 25	45 ± 10	
$S_{11}(1650)$	1727	1678	200	73	24
****		1655 ± 10	165 ± 20	77 ± 17	
$D_{15}(1675)$	1710	1670	154	18	49
****		1675 ± 5	147 ± 17	40 ± 5	
$F_{15}(1680)$	1748	1687	156	67	7.9
****		1685 ± 5	130 ± 10	67 ± 2	
$D_{13}(1700)$	1753	1747	156	5	-1
***		1700 ± 50	100 ± 50	10 ± 5	
$P_{11}(1710)$	1798	1803	508	32	40
***		1710 ± 30	180 ± 100	15 ± 5	
$P_{13}(1720)$	1725	1711	278	13	0
****		1725 ± 25	225 ± 75	15 ± 5	
$P_{13}(1900)$	1922	1861	1000	18	-3.5
**		1879 ± 17	498 ± 78	26 ± 6	
$F_{15}(2000)$	1928	1926	58	4	18
**		1903 ± 87	490 ± 310	8 ± 5	
$D_{13}(2080)$	1972	1946	494	15	5
**		1804 ± 55	450 ± 185	~ 4	
S_{11}(new)	1803	1878	508	41	-5
$S_{11}(2090)$	2090	2124	388	37	-18
*		2180 ± 80	350 ± 100	18 ± 8	
$P_{11}(2100)$	2196	2247	1020	42	32
*		2125 ± 75	260 ± 100	12 ± 2	
D_{13} (new)	2162	2152	292	14	7
P_{13} (new)	2220	2204	406	15	-4
$D_{15}(2200)$	2300	2286	532	16	8
**		2180 ± 80	400 ± 100	10 ± 3	

parameters in all channels up to the F waves and for energies less than 2 GeV. The results for the real and imaginary parts of the partial wave amplitudes $t_{\pi N}$ are shown in Figs. 3–6. The solid lines are the best fit within our model, while the dashed lines correspond to the nonresonant background $\tilde{t}_{\pi N}^B$ of Eq. (22). The open circles represent the partial wave analysis results of Ref. [34]. These figures show an excellent description of both the real and imaginary parts of the pion-nucleon scattering amplitudes in all cases except for the D_{35} and F_{17} channels. For the D_{35} channel, our problem lies mostly within the real part, as seen in Fig. 5. For the F_{17} channel in Fig. 6, the inclusion of further resonances does not improve the nonresonant background shown by the data, neither for the real nor for the imaginary part of the scattering amplitude.

B. Resonance parameters

Let us now look at the resonance parameters whose determination was one of the main issues of our investigation. Before going into detail by comparing our data with the Particle Data Group (PDG) values, we point out that our data analysis requires four very broad resonances, $S_{11}(1878)$, $D_{13}(2152)$, $P_{13}(2204)$, and $P_{31}(2100)$, states that are not in the current listing of the PDG [35]. Furthermore, we cannot remove the discrepancy between the background contributions and the data in the F_{17} channel by adding the $F_{17}(1990)$ resonance listed by the PDG, which is in line with the results of the SAID analysis [34].

The physical mass M_R, total width Γ_R, single-pion branching ratio $\beta_R^{1\pi}$, and background phase ϕ_R defined for each

TABLE II. Same as Table I, but for isospin-3/2 resonances.

N^*	$M_R^{(0)}$	M_R	Γ_R	$\beta_R^{1\pi}(\%)$	ϕ_R (deg)
$P_{33}(1232)$	1425	1233	132	100	12
****		1232 ± 1	118 ± 2	100	
$P_{33}(1600)$	1575	1562	216	6	−9
***		1600 ± 100	350 ± 100	17 ± 7	
$S_{31}(1620)$	1654	1616	160	32	−41
****		1630 ± 30	142 ± 18	25 ± 5	
$D_{33}(1700)$	1690	1650	260	15	−5
****		1710 ± 40	300 ± 100	15 ± 5	
$P_{31}(1750)$	1765	1746	554	4	−24
*		1744 ± 36	300 ± 120	8 ± 3	
$S_{31}(1900)$	1796	1770	430	8	−44
**		1900 ± 50	190 ± 50	2 ± 1	
$F_{35}(1905)$	1891	1854	534	11	−12
****		1890 ± 25	335 ± 65	12 ± 3	
$P_{31}(1910)$	1953	1937	226	14	−21
****		1895 ± 25	230 ± 40	22 ± 7	
$P_{33}(1920)$	1856	1827	834	12	3
***		1935 ± 35	220 ± 70	12 ± 7	
$D_{35}(1930)$	2100	2068	426	15	−20
***		1960 ± 60	360 ± 140	10 ± 5	
$D_{33}(1940)$	2100	2092	310	6	−10
*		2057 ± 110	460 ± 320	18 ± 12	
$F_{37}(1950)$	1974	1916	338	47	13
****		1932 ± 17	285 ± 50	40 ± 5	
$F_{35}(2000)$	2277	2260	356	11	−26
**		2200 ± 125	400 ± 125	16 ± 5	
P_{31} (new)	2160	2100	492	35	−25
$S_{31}(2150)$	2118	1942	416	70	−44
*		2150 ± 100	200 ± 100	8 ± 2	

overlapping nucleon resonance R were determined from Eqs. (28), (29), (42), and (43). The results are presented in Tables I and II for the isospin-$\frac{1}{2}$ and isospin-$\frac{3}{2}$ resonances, respectively. Using the speed-plot technique, we also calculated the resonance pole positions in the complex energy plane and the complex residues at these poles. The results are listed in Tables III and IV for the isospin-$\frac{1}{2}$ and isospin-$\frac{3}{2}$ resonances, respectively. In Tables I–IV, we also compare our results with the listings of the PDG.

1. S waves

As reported in Ref. [18], we need four S_{11} resonances to fit the πN scattering amplitude in this channel, instead of the three resonances listed by the PDG. The additional resonance $S_{11}(1878)$ was found to play an important role in pion photoproduction as well [18], but it was not seen in either the $\pi N \to \eta N$ reaction or recent measurements of η photoproduction from the proton [36]. There also arise some differences in the resonance parameters between our present results and those given by Ref. [18] because of the different definitions for the resonance masses and widths explained in the previous text. It turns out that the choice of these definitions has little effect on the extracted masses of all four S_{11} resonances. However, the extracted widths for the first and third resonances depend very much on the definitions, which leads to increased widths over those obtained in earlier work, i.e., from 90 to 130 MeV and from 265 to 508 MeV, respectively. Our results obtained for the pole position via the speed-plot technique generally agree with the PDG values for the real parts of the pole positions. However, we obtain much smaller values for the imaginary parts of the pole positions and for the residues at the pole.

For the isospin-3/2 channel, our extracted masses and widths differ from the PDG values by more than 100 MeV, all except the first resonance, $S_{31}(1620)$. The values obtained for the pole positions agree with the PDG values for the lower resonances. However, the imaginary part of the pole position for the $S_{31}(1900)$ and its residue at the pole comes out very small.

2. P waves

For P waves with isospin-1/2, our results are in good agreement with the PDG values regarding both pole positions and residues. However, the extracted widths are much larger than the corresponding PDG values. We also need an extra

TABLE III. Pole positions $W_p - \frac{1}{2}i\Gamma_p$ and absolute values of the residues $|\,r\,|$ at the pole, all in MeV, as well as the phases θ of the residues for isospin-1/2 resonances, as obtained from speed plots. Notation same as in Table I.

N^*	W_p	Γ_p	$\mid r \mid$	θ (deg)
$P_{11}(1440)$	1366	179	47	-87
****	1365 ± 15	190 ± 30	46 ± 10	-100 ± 35
$D_{13}(1520)$	1516	123	40	-6
****	1510 ± 5	114 ± 10	35 ± 3	-10 ± 4
$S_{11}(1535)$	1449	67	11	-46
****	1510 ± 20	170 ± 80	96 ± 63	15 ± 45
$S_{11}(1650)$	1642	97	21	-73
****	1655 ± 15	165 ± 15	55 ± 15	-75 ± 25
$D_{15}(1675)$	1657	132	24	-22
****	1660 ± 5	137 ± 12	29 ± 6	-30 ± 10
$F_{15}(1680)$	1663	115	38	-28
****	1672 ± 8	122 ± 12	38 ± 6	-23 ± 7
$D_{13}(1700)$	not seen	not seen	not seen	not seen
***	1680 ± 50	100 ± 50	6 ± 3	0 ± 50
$P_{11}(1710)$	1721	185	5	-163
***	1720 ± 50	230 ± 150	10 ± 4	-175 ± 35
$P_{13}(1720)$	1683	239	15	-64
****	1675 ± 15	195 ± 80	13 ± 7	-139 ± 51
$P_{13}(1900)$	1846	180	7	-75
**	not listed	not listed	not listed	not listed
$F_{15}(2000)$	1931	62	1.3	-272
**	not listed	not listed	not listed	not listed
$D_{13}(2080)$	1834	210	13	-134
**	1950 ± 170	200 ± 80	27 ± 22	~ 0
$S_{11}(2090)$	2065	223	16	-138
*	2150 ± 70	350 ± 100	40 ± 20	0 ± 90
$P_{11}(2100)$	1869	238	7	-216
*	2120 ± 240	240 ± 80	14 ± 7	35 ± 35
$D_{15}(2200)$	2188	238	21	-27
**	2100 ± 60	360 ± 80	20 ± 10	-90 ± 50

resonance $P_{13}(2204)$ in order to fit the scattering amplitude in this channel.

For the isospin-3/2 resonances $P_{31}(1750)$ and $P_{33}(1920)$, we extract widths of about 500 and 800 MeV, respectively, both very much above the PDG values. On the other hand, the residue and the imaginary part of the pole position for $P_{31}(1750)$ comes out much below the PDG listings.

3. D waves

For D waves with isospin-1/2 and isospin-3/2, our resonance parameters generally agree with the PDG values, except that we do not find a pole corresponding to $D_{13}(1700)$.

4. F waves

Even though we cannot describe the F_{17} channel, our results for the F-wave resonance parameters are in good agreement with the PDG listings.

TABLE IV. Same as Table III, but for isospin-3/2 resonances.

N^*	W_p	Γ_p	$\mid r \mid$	θ (deg)
$P_{33}(1232)$	1218	89	42	-35
****	1210 ± 1	100 ± 2	53 ± 2	-47 ± 1
$P_{33}(1600)$	1509	236	35	-197
***	1600 ± 100	300 ± 100	17 ± 4	-150 ± 30
$S_{31}(1620)$	1598	136	22	-99
****	1600 ± 10	118 ± 3	16 ± 3	-110 ± 20
$D_{33}(1700)$	1609	133	9.5	-52
****	1650 ± 30	200 ± 40	13 ± 3	-20 ± 25
$P_{31}(1750)$	1729	70	1	-123
*	1748	524	48	158
$S_{31}(1900)$	1775	36	1	-166
**	1870 ± 40	180 ± 50	10 ± 3	-20 ± 40
$F_{35}(1905)$	1771	190	11	-47
****	1830 ± 5	280 ± 20	25 ± 8	-50 ± 20
$P_{31}(1910)$	1896	130	6	-118
****	1880 ± 30	200 ± 40	20 ± 4	-90 ± 30
$P_{33}(1920)$	2149	400	38	-59
***	1900 ± 50	300 ± 100	24 ± 4	-150 ± 30
$D_{35}(1930)$	1992	270	18	-75
***	1900 ± 50	265 ± 95	18 ± 6	-20 ± 40
$D_{33}(1940)$	2070	267	7	-31
*	1900 ± 100	200 ± 60	24 ± 4	135 ± 45
$F_{37}(1950)$	1860	201	43	-45
****	1880 ± 10	240 ± 20	50 ± 7	-33 ± 8
$F_{35}(2000)$	2218	219	11	-36
**	2150 ± 100	350 ± 100	16 ± 5	150 ± 90
$S_{31}(2150)$	2012	148	6	-155
*	2140 ± 80	200 ± 80	7 ± 2	-60 ± 90

V. SUMMARY AND CONCLUSION

In earlier work, we constructed a meson-exchange model for the πN interaction which describes the πN elastic scattering data up to a pion laboratory energy of 400 MeV [10,14]. Our approach was based on a three-dimensional reduction scheme of the Bethe-Salpeter equation for a model Lagrangian involving π, N, Δ, σ, and ρ fields. This model was later extended to energies up to 2 GeV in the S_{11} channel by explicitly including the ηN channel and several higher resonances [18]. The influence of the 2π channels was accounted for by adding a phenomenological term in the resonance propagator. Good agreement was obtained with the data from the $\pi N \to \eta N$ reaction and pion photoproduction.

In the present work, the hadron-exchange coupled-channels model has been further extended to energies of 2 GeV and partial wave channels including the F waves. We have assumed that all the resonances observed in πN scattering are fundamentally three-quark states dressed by the coupling to the meson-nucleon continuum. Using such a scheme, we achieved a very good description of the πN elastic scattering amplitudes in all the partial waves and over the energy range up to 2 GeV, except for the F_{17} channel. However, the fit to the data requires four additional resonances with very large widths, $S_{11}(1878)$, $D_{13}(2152)$, $P_{13}(2204)$, and $P_{31}(2100)$, which are not listed by the PDG [35]. The first of these resonances, $S_{11}(1878)$, was also found in our previous

work [18], where a self-consistent analysis of pion scattering and pion photoproduction within a coupled-channels dynamical model was carried out for the S_{11} channel. The other three resonances, all with large widths, might be the artifacts of the oversimplification of our background contributions where, for example, the u-channel resonance excitations have been consistently neglected.

We have developed a scheme to extract the parameters of overlapping resonances in a completely symmetrical way with respect to the resonances. This scheme allows us to include the dressing of each particular resonance due to all the other resonances in the same channel. We have chosen to define the resonance energy such that the effect of vertex dressing is not included in the self-energy of a resonance, contrary to many previous investigations. Furthermore, the pole positions and the residues of the scattering amplitudes at the pole have been determined by means of the speed-plot technique. The comparison of the extracted resonance parameters with the PDG values indicates a qualitative agreement in general, but considerable discrepancies occur in some cases, particularly for the widths and residues of some higher resonances. Further investigations will be necessary to understand these differences in detail.

The πN model developed in this work will be used to study the meson cloud effects on the electromagnetic transition form factors of the higher resonances. It will also allow us to extract the helicity amplitudes of all resonances in a more consistent and reliable way.

ACKNOWLEDGMENTS

S.S.K. wishes to acknowledge the financial support from the National Science Council of ROC for his visits to the Physics Department of National Taiwan University. The work of S.N.Y. is supported in part by the NSC/ROC under Grant No. NSC095-2112-M022-025. We are also grateful for the support of the Deutsche Forschungsgemeinschaft through the SFB 443, by joint project NSC/DFG 446 TAI113/10/0-3 and by the joint Russian-German Heisenberg-Landau program.

[1] See, for example, S. Gasiorowicz, *Elementary Particle Physics* (Wiley, New York, 1966).
[2] S. N. Yang, J. Phys. G **11**, L205 (1985); Phys. Rev. C **40**, 1810 (1989).
[3] C. C. Lee, S. N. Yang, and T.-S. H. Lee, J. Phys. G **17**, L131 (1991); S. N. Yang, Chin. J. Phys. **29**, 485 (1991).
[4] T. Sato and T.-S. H. Lee, Phys. Rev. C **54**, 2660 (1996).
[5] S. S. Kamalov and S. N. Yang, Phys. Rev. Lett. **83** 4494 (1999).
[6] M. Lacombe, B. Loiseau, J. M. Richard, R. Vinh Mau, J. Conte, P. Pires, and R. deTourreil, Phys. Rev. C **21**, 861 (1980).
[7] R. Machleidt, K. Holinde, and Ch. Elster, Phys. Rep. **149**, 1 (1987).
[8] B. C. Pearce and B. Jennings, Nucl. Phys. **A528**, 655 (1991).
[9] F. Gross and Y. Surya, Phys. Rev. C **47**, 703 (1993).
[10] C. T. Hung, S. N. Yang, and T.-S. H. Lee, J. Phys. G **20**, 1531 (1994).
[11] C. Schütz, J. W. Durso, K. Holinde, and J. Speth, Phys. Rev. C **49**, 2671 (1994).
[12] A. D. Lahiff and I. R. Afnan, Phys. Rev. C **60**, 024608 (1999).
[13] V. Pascalutsa and J. A. Tjon, Phys. Rev. C **61**, 054003 (2000).
[14] C. T. Hung, S. N. Yang, and T.-S. H. Lee, Phys. Rev. C **64**, 034309 (2001).
[15] A. M. Gasparyan, J. Haidenbauer, C. Hanhart, and J. Speth, Phys. Rev. C **68**, 045207 (2003).
[16] H. Polinder and Th. A. Rijken, Phys. Rev. C **72**, 065210 (2005); **72**, 065211 (2005).
[17] M. Cooper and B. Jennings, Nucl. Phys. **A500**, 553 (1989).
[18] G. Y. Chen, S. Kamalov, S. N. Yang, D. Drechsel, and L. Tiator, Nucl. Phys. **A723**, 447 (2003).
[19] M. F. M. Lutz and E. E. Kolomeitseiv, Nucl. Phys. **A700**, 193 (2002); **A706**, 431 (2002); E. E. Kolomeitseiv and M. F. M. Lutz, Phys. Lett. **B585**, 243 (2004).
[20] C. Schütz, J. Haidenbauer, J. Speth, and J. W. Durso, Phys. Rev. C **57**, 1464 (1998).
[21] O. Krehl, C. Hanhart, C. Krewald, and J. Speth, Phys. Rev. C **62**, 025207 (2000).
[22] S. S. Kamalov, S. N. Yang, D. Drechsel, O. Hanstein, and L. Tiator, Phys. Rev. C **64**, 032201(R) (2001).
[23] V. Pascalutsa, M. Vanderhaeghen, and S. N. Yang, Phys. Rep. **437**, 125 (2007).
[24] R. Blankenbecler and R. Sugar, Phys. Rev. **142**, 1051 (1966).
[25] J. D. Bjorken and S. D. Drell, *Relativistic Quantum Mechanics* (McGraw-Hill, New York, 1964).
[26] S. Morioka and I. R. Afnan, Phys. Rev. C **26**, 1148 (1982); B. C. Pearce and I. R. Afnan, *ibid*. **34**, 991 (1986).
[27] L. Tiator, C. Bennhold, and S. S. Kamalov, Nucl. Phys. **A580**, 455 (1994).
[28] A. I. L'vov, V. A. Petrun'kin, and M. Schumacher, Phys. Rev. C **55**, 359 (1997).
[29] D. Drechsel, O. Hanstein, S. S. Kamalov, and L. Tiator, Nucl. Phys. **A645**, 145 (1999).
[30] S. Morioka and I. R. Afnan, Phys. Rev. C **26**, 1148 (1982); B. C. Pearce and I. R. Afnan, *ibid*. **34**, 991 (1986).
[31] M. L. Goldberger and K. M. Watson, *Collision Theory* (Wiley, New York, 1964).
[32] G. Höhler and A. Schulte, πN Newslett. **7**, 94 (1992); G. Höhler, *ibid*. **9**, 1 (1993).
[33] O. Hanstein, D. Drechsel, and L. Tiator, Phys. Lett. **B385**, 45 (1996).
[34] R. A. Arndt, W. J. Briscoe, I. I. Strakovsky, R. L. Workman, and M. M. Pavan, Phys. Rev. C **69**, 035213 (2004); R. A. Arndt, W. J. Briscoe, I. I. Strakovsky, and R. L. Workman, *ibid*. **74**, 045205 (2006).
[35] W.-M. Yao, J. Phys. G **33**, 1 (2006).
[36] U. Thoma, Int. J. Mod. Phys. A **20**, 1568 (2005); D. Elsner *et al*., Eur. Phys. J. (to be published), nucl-ex/0702032.